TECHNICAL
LIBRARY

TECHNICAL REPORT ARLCD-TR-80017

EVALUATION OF PROPELLANT EROSIVITY WITH VENTED EROSION APPARATUS

A. J. BRACUTI
L. BOTTEI
J. A. LANNON
ARRADCOM

L. H. CAVENY
PRINCETON UNIVERSITY
PRINCETON, NJ 08540

MARCH 1981

US ARMY ARMAMENT RESEARCH AND DEVELOPMENT COMMAND
LARGE CALIBER
WEAPON SYSTEMS LABORATORY
DOVER, NEW JERSEY

APPROVED FOR PUBLIC RELEASE; DISTRIBUTION UNLIMITED.

REPORT DOCUMENTATION PAGE		READ INSTRUCTIONS BEFORE COMPLETING FORM
1. REPORT NUMBER Technical Report ARLCD-TR-80017	2. GOVT ACCESSION NO.	3. RECIPIENT'S CATALOG NUMBER
4. TITLE *(and Subtitle)* EVALUATION OF PROPELLANT EROSIVITY WITH VENTED EROSION APPARATUS		5. TYPE OF REPORT & PERIOD COVERED Final
		6. PERFORMING ORG. REPORT NUMBER
7. AUTHOR(s) A. J. Bracuti, L. Bottei, and J. A. Lannon, ARRADCOM L. H. Caveny, Princeton University		8. CONTRACT OR GRANT NUMBER(s) 1L162603AH18/TAR/WAO3
9. PERFORMING ORGANIZATION NAME AND ADDRESS ARRADCOM, LCWSL Applied Sciences Division (DRDAR-LCA-G) Dover, NJ 07801		10. PROGRAM ELEMENT, PROJECT, TASK AREA & WORK UNIT NUMBERS
11. CONTROLLING OFFICE NAME AND ADDRESS ARRADCOM, TSD STINFO Division (DRDAR-TSS) Dover, NJ 07801		12. REPORT DATE MARCH 1981
		13. NUMBER OF PAGES 50
14. MONITORING AGENCY NAME & ADDRESS*(if different from Controlling Office)*		15. SECURITY CLASS. *(of this report)* Unclassified
		15a. DECLASSIFICATION/DOWNGRADING SCHEDULE

16. DISTRIBUTION STATEMENT *(of this Report)*

Approved for public release; distribution unlimited.

17. DISTRIBUTION STATEMENT *(of the abstract entered in Block 20, if different from Report)*

18. SUPPLEMENTARY NOTES

19. KEY WORDS *(Continue on reverse side if necessary and identify by block number)*

Wear	Triple-base propellant
Erosion	Erosivity
RDX composite propellant	
Double-base propellant	

20. ABSTRACT *(Continue on reverse side if necessary and identify by block number)*

Gun steel erosion studies were performed using three propellant types (double-base, triple-base, and RDX composite), each formulated to have isochoric flame temperatures of approximately 2700 K, 3000 K, and 3300 K, respectively. These erosion studies were performed independently at ARRADCOM and Princeton University in different erosion vent apparatuses. At ARRADCOM, the erosivities of propellant types at equivalent temperatures were evaluated on the basis of equal charge weights, peak pressures, and energy. The nitramine composite propellants in the 280 MPa regime were the most erosive at all flame   (Continued)

DD FORM 1473   EDITION OF 1 NOV 65 IS OBSOLETE

20. ABSTRACT (Continued)

temperatures. Within a propellant type, erosivity increased with flame temperature. In the lower pressure regime (approximately 210 MPa), the general erosivity levels were lower for all propellants. At the lower temperatures the nitramine composites were the most erosive, but at 3300 K the erosivities were approximately the same for each propellant. At the high pressures, the dominant factor in erosivity is propellant gas composition which determines the heat convection to the barrel surface. At the lower pressure, gas composition is the dominant erosion factor at 2700 K and 3000 K, but at 3300 K the flame temperature becomes the dominant factor.

The two erosion apparatuses gave similar results, but where differences occurred, no explanation was available.

ACKNOWLEDGMENTS

CONTENTS

TABLES

FIGURES

INTRODUCTION

The demand for weapon systems with greater ranges and higher muzzle velocities has created the need for higher force propellants. Sufficient force can be attained with conventional nitrate-ester propellant formulations (double base and triple base nitrate-ester types), but the isochoric flame temperature increases accordingly. Since high flame temperatures aggravate gun barrel erosion, alternate low flame temperature propellants have been sought.

Nitramine composite propellants (e.g., RDX formulations) have lower flame temperatures than energetically comparable nitrate-ester propellants. With nitramine and nitrate-ester propellants displaying equivalent flame temperatures, the nitramine propellants are more energetic and, consequently, appear to be candidate propellants for providing increased energy at lower flame temperatures.

Despite the fact that nitramine propellants have lower flame temperatures, there is some evidence that nitramines are more erosive to gun steel than conventional propellants (ref 1). This suggests that factors other than isochoric flame temperature play a signifiant role in the erosion mechanism. Experiments in which either the propellant formulation or the pressure-versus-time (p-vs-t) cycle are changed for the purpose of evaluating their influence on steel erosion always produce interactions which complicate the interpretation of the specific effects which produce erosion. For example, changes in propellant formulation may significantly alter both the propellant burning rate and the combustion gas composition which affects the rate at which the steel is heated. Convective heating rates are very dependent on propellant flame temperatures as well as gas transport properties. Differences in erosion as a function of propellant type must be interpreted in terms of gas composition in order to analyze the contributions of chemical interactions which produce changes in transport properties such as thermal conductivity and specific heat (ref 2).

To define more clearly the intrinsic erosivities of energetically comparable propellants and the role of propellant flame temperature in the erosion process, a representative series of double base, triple base, and RDX composite propellants were selected in which each propellant type was formulated to burn at 2700K, 3000K, and 3300K. Each propellant web thickness was selected so that the burning time would be in the same range. The compositions of these

propellants and related physicochemico properties are presented in table 1.

Experiments performed on these nine propellants at ARRADCOM and at Princeton University are described in this report and the results compared.

EXPERIMENTAL PROCEDURES

ARRADCOM Experiments

The erosion data were obtained by means of a closed bomb modified to accept a gun barrel and a steel erosion sleeve, which is referred to as the vented erosion tester (refs 3 and 4, fig. 1). The erosion sleeves consisted of AISI 4340 steel having an outer diameter of 2.70 cm, an inner diameter of 0.95 cm, a length of 2.064 cm, and a mass of approximately 80 grams. A pressure transducer positioned inside the closed bomb was connected to a Nicolet digital oscilloscope which was scaled to display pressure-versus-time. To control pressure, a stainless steel rupture disc was inserted between the barrel and the steel erosion sleeve and the barrel was filled with water to insure proper pressure buildup.

Each sleeve was weighed before testing, fired with three shots, cleaned, and reweighed. After three firings, the average weight loss was used as a measure of propellant erosivity; pressure and burntime measurements were also recorded and averaged. Propellant charge weights ranged from 24 grams to 52 grams.

The internal ballistics were controlled by arbitrarily adjusting the charge weights. The controlled independent variables were the flame temperature and the propelling charge weight, while the experimentally measured dependent variables were burntime, pressure, and sleeve mass loss (erosion). The nitramine propellants were the slowest burning and, in order to obtain similar burntimes, it was sometimes necessary to grind the propellants.

In the first series of tests, propelling charges of equal weight (38 g) were fired in the test fixture to compare the relative erosivities on a fixed weight basis.

In a second series of tests, the propelling charge weights were selected so that each propellant produced approximately the same peak pressure. Comparisons were made at approximately 280 MPa and 210 MPa.

2

A third set of tests were conducted in which the charge weights were adjusted to give each propellant approximately the same energy (4.88 x 10⁵ joules), similar to the way propellants would be substituted in a gun system. When the propellant is replaced in a gun tube with a given muzzle velocity, the webs are adjusted to obtain a given pressure, and propellant weights are adjusted to give equivalent energy output. Propellant type erosivities were compared on the basis of equal propelling charge weights, peak pressure, and energy output.

Princeton University Experiments[1]

Erosion of steel specimens was produced using a vented combustor (fig. 2). Specimens for erosion measurements were AISI 4340 steel 2.5 mm thick and 0.17 mm diameter orifices and the leading edge of the orifice was streamlined. The p-vs-t cycles produced in the combustor approximate those produced by large gun chambers. The primary measurement in these experiments was mass loss. A mass loss of 1 mg corresponds to an equivalent erosion depth of about 22 micrometers along the orifice. The propelling charge weights during the test series range from 0.6 grams to 1.4 grams.

The Princeton group used the basis for comparing propellant erosivity given below. Since the net effect of the imposed p-vs-t program is to accelerate a projectile in a barrel, an effective measure of the relative energy associated with a particular program is the velocity it would impart to a projectile. Without regarding barrel length and neglecting losses, projectile velocity is approximately proportional to the integral of pressure over the action time. For a given p-vs-t program, the relative energy associated with a particular duty cycle can be calculated without knowing the specifics of the gas composition, flame temperature, burning rate, surface area, etc.

Another important factor in determining the relative erosivities of various propellants and p-vs-t programs is the dynamics of the propellant gases heating the steel surface and the conduction of heat to the subsurface regions. For example, if a prescribed p-t integral (muzzle velocity) is achieved by using a relatively low pressure and an extended action time, the steel surface temperature can be maintained below the melting point where no significant mass loss occurs. This situation can occur because at sufficiently low

---

[1]Personal communication with L. Caveny, Princeton University, Princeton, NJ, August 1979.

pressures (low heating rates) there is ample time for heat to be conducted away from the steel surface; therefore, the surface temperature remains below the melting point. A comparison of relative erosivity must account for the dynamics of the heat transfer processes. Accordingly, the integral was evaluated between the times the pressure exceeded a threshold of 60 MPa, since below that pressure the low heating rates do not contribute significantly to the mass loss. The integral is referred to as I_{60}. In this manner the correlation is weighed toward that portion of the heating cycle which produces erosion and away from the low pressure extended time p-vs-t programs that do not produce measurable mass losses.

While it is reasonable to compare the relative erosivities of propellants with equal muzzle velocities, it is the combined propellant and grain geometry systems which are being compared rather than the propellants alone. Since propellant properties (such as burning rate) and grain geometry characteristics (such as web thickness) affect the p-vs-t history, separating the propellant effects from the grain geometry effects would require additional experiments in which the propellant formulations are held constant and grain geometry systematically varied.

RESULTS

The ARRADCOM erosion results are shown in table 2 where mass losses are given at equal charge weights for the nine propellants; in table 3, mass losses at equal pressures; and in table 4, mass losses at equal energy. As expected, the erosion increases proportionately with the flame temperature and the mass losses for the double base, triple base, and nitramine propellants are different functions of increasing temperatures.

The Princeton University results are summarized in tables 5, 6 and 7. Specimen-to-specimen variation can be observed by comparing the mass losses of specimens 1 and 2. This type of variation is typical of that observed in the previous eperimental series. The fourth test in each series was performed after the results of the first three tests were analyzed and the test conditions were selected to resolve ambiguities and broaden data correlations. The p-vs-t integrals were measured with a planimeter on the oscilloscope photographic records and were accurate to within 3%.

4

Each of the 72 measured mass losses are plotted on mass loss versus I_{60} plots (figs. 3 through 5) and least-squares lines were placed through the points (table 8). A few of the data points were excluded from the correlations, since they were exceptions to general trends (table 8). The relative erosivity of a particular propellant grain type increased with increasing flame temperature. The increase in mass loss produced by going from 3000 K to 3300 K tends to be greater than that produced by going from 2700 K to 3000 K; however, at the lower I_{60} values, the trends with increasing temperature are less distinct.

The results of figures 6 through 8 are taken from tables 5 through 7 and compare the three propellant types at the same nominal flame temperatures. The grains containing RDX produce higher mass losses at every temperature; however, the higher erosivity becomes more prominent as flame temperature increases. The mass loss differences produced by double- and triple-base grains are less distinct and tend to be similar. The mass loss data were plotted as a function of peak pressure (figs. 9 through 11), and lines through the data were visually determined. The fact that the results are systematic and reveal the same trends as those illustrated in figures 6 through 8 is a result of the efforts to make the web burning times equal. For example, propellant grains which produced equivalent peak pressure at one-half of the burning time would produce greatly reduced mass losses.

DISCUSSION

ARRADCOM Results

In comparing propellant types on an equal charge weight basis, the data presented in table 2 reveal that the peak pressures for double- and triple-base propellants are equivalent over the entire temperature range, since the number of moles of gas evolved per unit mass of propellant is approximately the same in each case (table 1). Although the burning times for the two propellant types are equivalent in both the 2700 K and 3000 K flame temperature regions, the burning time of the triple-base propellant at 3300 K is about 9% longer than the comparable double-base propellant. A comparison of their respective erosivities indicates that double- and triple-base propellants have similar erosivities in the 2700 K and 3000 K regions. This may be due to increased burntime.

5

The nitramine composite propellants display higher pressures and longer burntimes than the double- and triple-base propellants. In the 2700 K and 3000 K regions, the nitramine composite propellants are more erosive than the other types, while in the 3300 K region they are about as erosive as the triple-base type and 30% more erosive than the double base. This correlates with the respective burntimes of the propellants and suggests that, for a given flame temperature and peak pressure, erosivity increases with burntime. The longer burntimes probably have a greater influence at the higher flame temperatures since the steel bore surface would be at an elevated temperature for a greater period of time.

The nitramine composites are more erosive at equal peak pressure in the 280 MPa region than either double- or triple-base propellants at all flame temperatures. It is also evident that double- and triple-base propellants have similar erosivities; the double-base propellant is slightly more erosive at 2700 K and 3000 K, and the triple-base propellant is more erosive at 3300 K.

Although it is apparent tht erosion increases with flame temperature, the trends are not analogous among the propellant types. With double- and triple-base propellants, erosivity increases approximately 100% with each 3000 K increase in flame temperature. The 3000-K nitramine composite propellant is 14% more erosive than the 2700 K formulation, while the 3300 K nitramine composite propellant exhibits a 50% increase in erosivity over the 3000-K formulation. This may mean that the erosion threshold of steel (the point where the conditions for erosion of steel are optimized) is exceeded at a lower flame temperature for the nitramine composite than for either the double- or triple-base propellant.

In contrast to the equal weight data, the burntimes within each group are relatively constant with average values of 3.6 ms, 3.7 ms, and 4.0 ms for double base, triple base, and nitramine composite propellants, respectively. Burntimes do not play a significant role in data variation. Since the propellants are compared on the basis of equivalent temperature and pressure, the quantity of gases is also equivalent; the composition of these gases appears to be the determining factor in the observed erosion at 280 MPa.

In the 210 MPa peak pressure range all propellant types are less erosive than observed in the 280 MPa peak pressure range. Nitramine composite propellant are more erosive than their counterparts at 2700 K and 3000 K, while the 3300 K nitramine composite propellants are about as erosive as the 3300 K triple-base type,

6

but more erosive than the 3300 K double-base formulation. Double- and triple-base propellant have comparable erosivities at 2700 K and 3000 K, but at 3300 K the triple base is about 70% more erosive. The double- and triple-base types display a 100% increase in erosivity going from the 2700 K to 3000 K formulations. The 3300 K double-base propellant is 360% more erosive than the 3000 K formulation, while 3300 K triple base is 680% more erosive than the 3000 K formulation. The nitramine composite types are initially more erosive and the increase in erosivity with temperature is not as large. For example, 3000 K nitramine composite is 40% more erosive than that at 2700 K and 3300 K nitramine composite is 60% more erosive than that at 3000 K.

These data suggest that the erosion process at high pressure and high flame temperature differs from that occurring at low pressure and high flame temperature. The erosion threshold of steel may be exceeded by all the propellants at 3300 K and by only the nitramine composites at 2700 K and 3000 K.

The relationship between peak pressure and erosivity are illustrated in figures 12, 13, and 14 in which isothermal peak pressure for each propellant is plotted as a function of mass loss (erosivity).

At equal propellant energies in the lower pressure regime (210-220 MPa), double- and triple-base propellants display similar erosivity profiles over the entire flame temperature range. The nitramine composites have comparable erosivity only at 3300 K and are more erosive at 2700 K and 3000 K. The data support the contention that the low pressure, high temperature (3300 K) erosion process differs from the high pressure, high temperature process.

In the higher pressure range (250 MPa 250 to 280 MPa), nitramine propellants are more erosive at all flame temperatures. Although the double-base propellants are about twice as erosive as triple-base propellants at 2700 K and 3000 K; both types have equivalent erosivities at 3000 K.

The experimental results indicate that, regardless of temperature, nitramine composite propellants are more erosive than double- or triple-base propellants in 280 MPa pressure range. Erosivity increases with flame temperature and peak pressure within each propellant type. On comparing propellant erosivities of the basis of equal weight, energy, and pressure, it is evident that the rate of erosion depends on the composition of the propellant gas. The nitramine composite propellants are most erosive because they produce combustion gases with the lowest average molecular weight and the highest thermal conductivity and lowest specific heats. This

7

is illustrated in figure 15 where erosivity is plotted against average molecular weight. Therefore, for any given flame temperature and burning time, nitramine composite propellants heat the barrel surface faster to a higher temperature resulting in greater erosion.

In the lower pressure range (210 MPa), nitramine composite propellants are more erosive than the double- and triple-base type at 2700 K and 3000 K, but at 3300 K all the propellants have approximately the same erosive behavior. This indicates that at the low pressure of 3300 K, propellant flame temperature not propellant gas composition is the dominant factor in the erosion process and is essentially consistent with the low pressure trends observed when comparing propellant erosivities on an equal pressure.

Princeton Results

The RDX composite grains are the most erosive for equivalent p-vs-t integrals, whereas there are no distinct differences in erosivity of the double- and triple-base grains.

The erosion data are generally correlated by the p-vs-t integral for pressure greater than 60 MPa.

Even though a relatively small data sample was taken, the trends are well defined. The specimen-to-specimen variations are an intriguing aspect of the results. Of the 26 specimen pairs, one-third had specimen-to-specimen differences of 0.5 mg or more. Since the two specimens in each experiment experience identical p-vs-t and combustion gas conditions, understanding the specimen-to-specimen differences is an integral part of understanding the overall erosion process. Note that the most homogeneous propellants, the double-base propellants, had the smallest specimen-to-specimen variations and the best coefficient of determinations.

Part of the research being conducted at Princeton University relates low rates of mass loss to water vapor where the steel surface remains below the melting temperature (ref 5). Under those conditions, the mass loss can be attributed to surface chemical attack. In the present test series, the mass loss is at a relatively high rate and is a result of high convective heating followed by melt and wipe-off. The arguments associated with water vapor concentration and the H_2O to H_2 ratio do not apply.

Explanations of the difference in erosion rates under similar p-vs-t programs require analyses that include the dynamics of the heat conduction processes, the effects of shifting equilibrium on transport properties, etc. (ref 2). However, it is interesting to

look for a simple correlation between nearly constant flame temperature and I_{60}. Those gases with the highest fraction of light molecular weight combustion products (or the lowest average molecular weight) have the highest thermal conductivities. For constant flame temperature (3300 K) and I_{60} (1.0 MP-s), mass loss increases as molecular weight decreases (fig. 15). Apparently, the desired low molecular weight for improved impetus produces a correspondingly larger increase in convective heating rate.

REFERENCES

1. B. D. Lehman, J. P. Picard, "Advanced Nitramine Propellant Formulations for Tank Ammunition," Proceedings of the Tri-Service Gun Tube Wear and Erosion Symposium, ARRADCOM, Dover, NJ, March 1977, pp 487-510.

2. L. H. Gaveny, A. Gany, M. Summerfield, and J. W. Johnson, "Effects of Propellant Type on Steel Erosion," Proceedings of JANNAF 1978 Propulsion Conference, CPIA Publication 293, vol V, February 1978, pp 285-299.

3. C. Lenchitz, R. W. Velicky, L. A. Bottei, and G. Silvestro, "Some Aspects of the Erosion Reducing Characteristics of the Titanium Oxide-Wax Additive," Technical Memorandum 1968, Picatinny Arsenal, Dover, NJ, November 1965.

4. C. Lenchitz, G. Silvestro, "A Study of the Erosion Process Using Several Group IV Oxides," Technical Memorandum 1869, Picatinny Arsenal, Dover, NJ, December 1968.

5. A. Gany, L. H. Caveny, and J. W. Johnson, "Erosion of Steel by Water-Vapor Containing High Temperature Flow," Non-Equilibrium Interfacial Transport Process, ASME, July 1979.

Table 1. Propellant compositions and physico-chemico properties[a]

	Double base			Triple base			RDX composite		
	1	2[b]	3	1	2[c]	3	1	2	3
Compositions (%)									
NC (13.25% N)	66.6	69.9	73.2	--	--	--	--	--	--
NC (12.6%)	--	--	--	27.4	27.4	27.4	30.0	30.0	30.0
NG	20.0	20.0	20.0	11.0	22.0	33.0	15.6	18.3	21.1
NG$_u$	--	--	--	59.6	48.6	37.6	--	--	--
RDX	--	--	--	--	--	--	41.5	41.5	41.5
EC	11.1	7.9	4.5	--	--	--	1.5	1.5	1.5
DOP	--	--	--	--	--	--	11.2	8.5	5.6
c_p (froz) (J/mol)	41.8	43.5	45.6	42.5	44.0	45.6	40.6	42.0	43.5
Calculated values									
t_f (K)	2705	2994	3297	2698	3004	3304	2708	3002	3307
I (J/g)	991	1046	1093	1007	1075	1132	1078	1143	1200
CO (mol/kg)	21.2	19.0	16.3	12.1	11.7	11.1	20.4	18.7	16.7
H_2	8.2	6.0	4.0	7.6	5.6	4.0	11.7	9.2	6.7
H_2O	6.8	8.3	9.4	9.4	10.5	11.2	6.1	7.6	8.9
N_2	4.9	5.0	5.0	13.4	12.1	10.7	8.0	8.2	8.4
CO_2	2.6	3.5	4.8	2.2	2.9	3.9	1.6	2.1	2.8
Total (mol/kg)	44.1	42.0	39.9	44.9	43.1	41.2	47.9	45.8	43.6
M_W (g/g-mol)	22.7	23.8	25.1	22.3	23.2	24.2	20.9	21.8	22.9
H_2O/H_2	0.83	1.38	2.35	1.24	1.88	2.80	0.52	0.83	1.33
Measured									
HEX	826	909	1005	862	928	1058	--	--	--
Web (in.)	0.023	0.026	0.034	0.020	0.034	0.021	0.025	0.030	--

a Calculated by Blake
b Similar to M26
c Similar to M30

11

Table 2. Equal charge weights*

Sample	Weight (g)	Flame temp (K)	Peak pressure (MPa)	Burning time (ms)	Erosion (mg/shot)
Double base	38.0	2705	210	4.8	0.4
		2705	209	4.8	0.6
		2705	209	4.8	1.0
		2994	213	4.6	2.4
		2994	213	4.6	1.6
		3297	226	4.5	16.6
		3297	225	4.4	15.5
Triple base	38.0	2698	211	5.0	0.7
		2698	210	4.8	1.5
		2698	209	4.6	1.7
		3004	214	4.6	2.8
		3004	213	4.8	3.0
		3304	224	4.7	25.3
		3304	227	4.8	20.9
Nitramine composite	38.0	2708	212	5.7	2.3
		2708	213	6.0	4.5
		3002	231	5.0	11.1
		3002	234	4.9	10.2
		3002	231	5.0	11.1
		3307	239	4.9	20.1
		3307	239	4.9	22.3

* Weight = 38.0 grams

12

Table 3. Equal peak pressure

Sample	Weight (g)	Flame temp (K)	Peak pressure (MPa)	Burning time (ms)	Erosion (mg/shot)
Double base	51.0	2705	278	3.6	9.3
	51.0	2705	277	3.6	8.0
	49.0	2994	275	3.6	16.2
	49.0	2994	275	3.6	13.0
	47.0	3297	276	3.7	26.9
	47.0	3297	272	3.6	29.3
Triple base	52.0	2698	276	3.6	5.9
	52.0	2698	276	3.7	7.2
	50.0	3004	277	3.8	11.9
	50.0	3004	276	3.7	14.4
	48.0	3304	276	3.8	33.8
	48.0	3304	275	3.8	31.9
Nitramine composite	48.0	2708	277	4.0	21.6
	48.0	2708	276	4.0	20.6
	46.0	3002	277	3.9	23.3
	46.0	3002	280	3.9	25.1
	44.0	3307	275	4.1	37.8
	44.0	3307	278	4.1	40.4
Double base	38.0	2705	209	4.8	0.6
	37.0	2994	211	5.0	1.4
	37.0	2994	211	5.0	1.4
	36.0	3297	210	4.9	6.5
Triple base	38.0	2698	211	5.0	0.7
	37.7	3004	209	5.0	1.4
	36.0	3304	212	5.1	10.9
Nitramine composite	38.2	2708	219	4.8	4.8
	38.0	2708	212	5.7	3.3
	36.0	3002	212	5.8	6.9
	34.0	3307	212	5.6	8.8
	34.2	3307	209	4.8	10.0

13

Table 4. Equal energy

Sample	Weight (g)	Flame temp (K)	Peak pressure (MPa)	Burning time (ms)	Erosion (mg/shot)
Double base	41.7	2705	219	4.6	0.7
	41.7	2705	220	4.5	1.9
	39.6	2994	219	4.5	1.9
	39.6	2994	214	4.7	2.5
	38.3	3297	214	4.6	10.6
	38.3	3297	216	4.5	9.5
Triple base	40.3	2698	213	4.5	2.0
	40.3	2698	213	4.5	1.7
	37.7	3004	209	5.0	1.4
	37.7	3004	209	5.0	2.0
	36.0	3304	211	5.1	9.5
	36.0	3304	210	5.1	9.2
Nitramine composite	38.2	2708	216	6.0	4.0
	48.2	2708	217	5.6	3.4
	35.9	3002	213	5.7	7.2
	35.9	3002	214	5.6	6.0
	34.2	3307	211	5.7	8.0
	34.2	3307	212	5.6	10.8
Double base	51.6	2705	278	3.5	9.1
	49.0	2994	275	3.6	14.6
	47.0	3297	274	3.7	27.6
Triple base	50.0	2698	261	3.7	4.9
	46.3	3004	255	3.9	8.5
	44.3	3304	254	4.0	26.3
Nitramine composite	47.0	2708	274	4.0	14.9
	43.6	3002	267	4.0	20.8
	42.3	3307	266	4.2	32.8

14

Table 5. Erosion produced by double-base propellant

Flame temp (K)	Test	Sample weight (g)	Peak pressure (MPa)	Mass loss (mg)		Pressure integral* (MPa-s)
				spec. 1	spec. 2	
2994	21	0.9872	238	2.30	2.77	0.978
2994	22	1.1122	290	3.60	4.00	1.111
2994	23	1.3030	362	5.36	5.28	1.178
2994	37	0.7776	162	1.00	0.80	0.716
2705	24	0.9861	224	2.43	2.66	0.917
2705	26	1.3973	379	4.31	4.87	1.210
2705	27	1.2589	317	3.45	3.69	1.033
2705	38	0.8280	176	0.74	0.92	0.797
3297	28	0.9875	231	4.14	4.33	0.890
3297	29	1.2162	317	6.08	6.47	1.006
3297	30	0.8342	159	2.42	2.98	0.619
3297	39	0.6090	117	0.81	0.64	0.474

*Integral is for time period when pressure exceeds 60 MPa.

Table 6. Erosion produced by triple-base propellant

Flame temp (K)	Test	Sample weight (g)	Peak pressure (MPa)	Mass loss (mg)		Pressure integral* (MPa-s)
				spec. 1	spec. 2	
3002	2	0.9825	214	1.31	2.20	0.958
3002	3	1.2445	310	3.28	3.25	1.187
3002	4	1.4150	379	3.90	4.18	1.159
3002	31	0.7480	145	0.81	0.65	0.469
2698	5	0.9868	204	1.37	1.36	0.883
2698	6	1.2440	331	3.26	2.32	1.241
2698	7	1.3769	344	4.00	3.52	1.257
2698	32	1.1133	269	2.07	1.90	1.149
3304	8	0.9700	231	4.24	3.58	0.909
3304	9	1.2002	314	6.58	5.36	1.009
3304	10	1.3907	386	7.81	8.65	1.115
3304	33	0.6645	128	2.08	1.76	0.549

* Integral is for time period when pressure exceeds 60 MPa.

Table 7. Erosion produced by nitramine propellant

Flame temp (K)	Test	Sample weight (g)	Peak pressure (MPa)	Mass loss (mg)		Pressure integral* (MPa-s)
				spec. 1	spec. 2	
3002	11	0.9817	248	3.87	3.41	0.875
3002	12	1.1987	341	4.93	5.58	1.078
3002	13	0.8369	176	2.09	2.06	0.527
3002	34	0.8800	203	2.30	2.91	0.840
2708	14	0.9878	234	2.07	1.91	0.897
2708	15	1.1177	300	3.21	3.20	1.076
2708	17	1.2414	355	4.45	4.30	1.078
2708	35	0.8991	200	2.25	2.22	0.812
3305	18	0.9859	248	6.16	5.60	0.881
3305	19	1.1672	321	8.30	6.60	1.009
3305	20	0.8388	186	4.98	4.48	0.701
3305	36	0.6492	117	1.73	1.68	0.479

* Integral is for time period when pressure exceeds 60 MPa.

17

Table 8. Regression analysis of data

Type of Propellant	Power curve $M = aI_{60}^b$			Linear regression $M = a + bI_{60}$			Flame temp (K)
	r^2	a	b	r^2	a	b	
Triple base	0.878	2.468	1.700	0.804	−1.397	4.081	3004
	0.979	1.638	1.495[a]	0.970	−0.876	2.526[a]	3004
	0.918	5.764	1.941	0.850	−4.237	10.323	3004
Nitramine composite	0.770	4.137	1.204	0.783	−1.222	5.561	3002
	0.718	3.078	2.168	0.704	−3.666	6.852	2708
	0.946	7.789	1.946	0.935	−3.074	10.45	3307
Double base	0.980	2.780	3.468	0.917	−5.699	8.856	2994
	0.854	2.647	3.966	0.939	−5.919	8.898	2705
	0.910	6.439	2.626[b]	0.951	−3.567	9.436	3297

Definitions:

r^2 is coefficient of determination.

I_{60} is pressure integral for the period in which
p is greater than 60 MPa.
M is mass loss in grams.

[a] Mass loss above 3.0 mg excluded from correlation.
[b] Data from test 29 excluded from correlation.

18
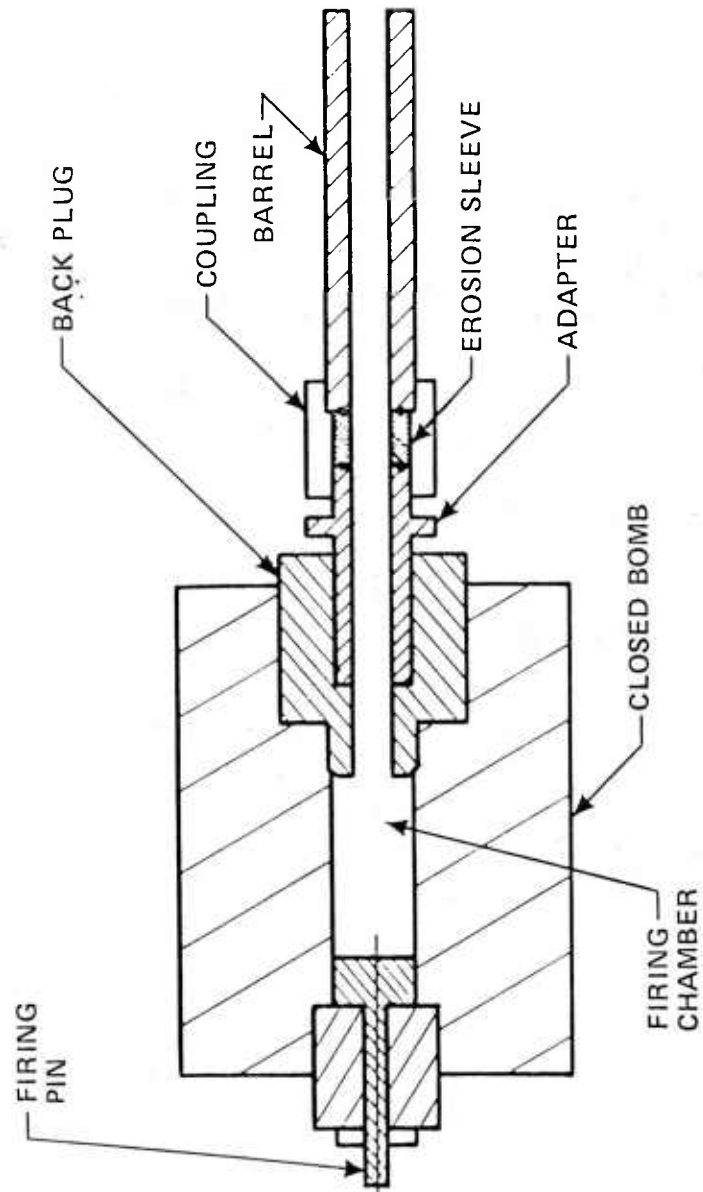
Figure 1. ARRADCOM vented erosion tester

19

RUPTURE DISK

SPECIMEN METAL DISK

RETAINER

PROPELLANT GRAIN
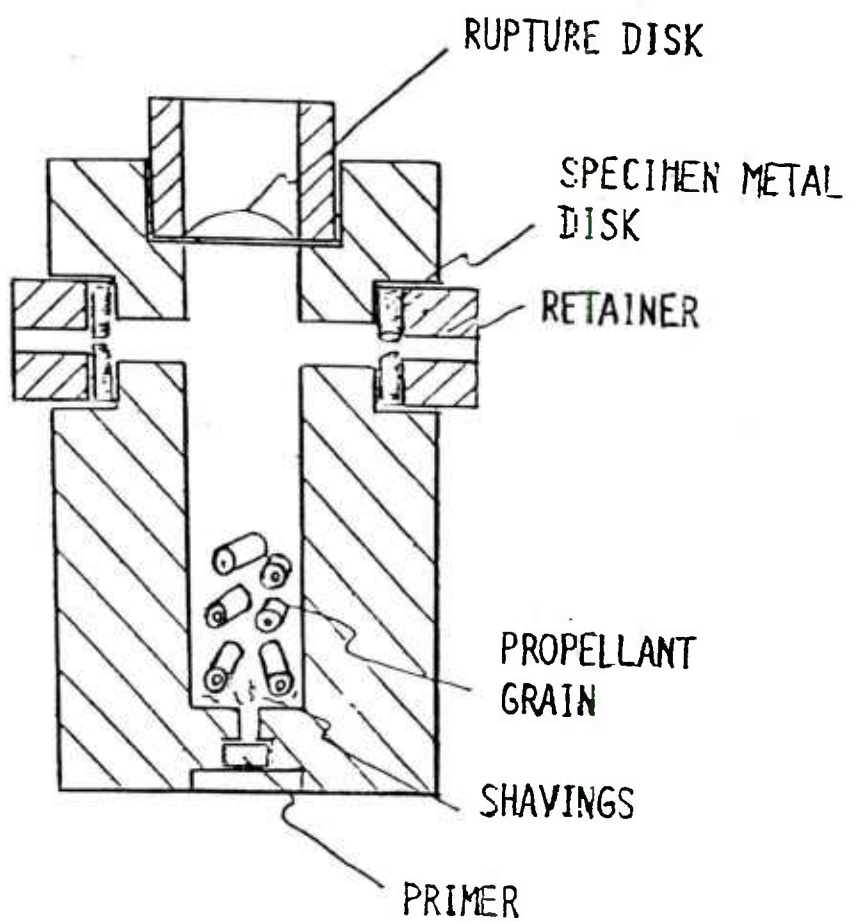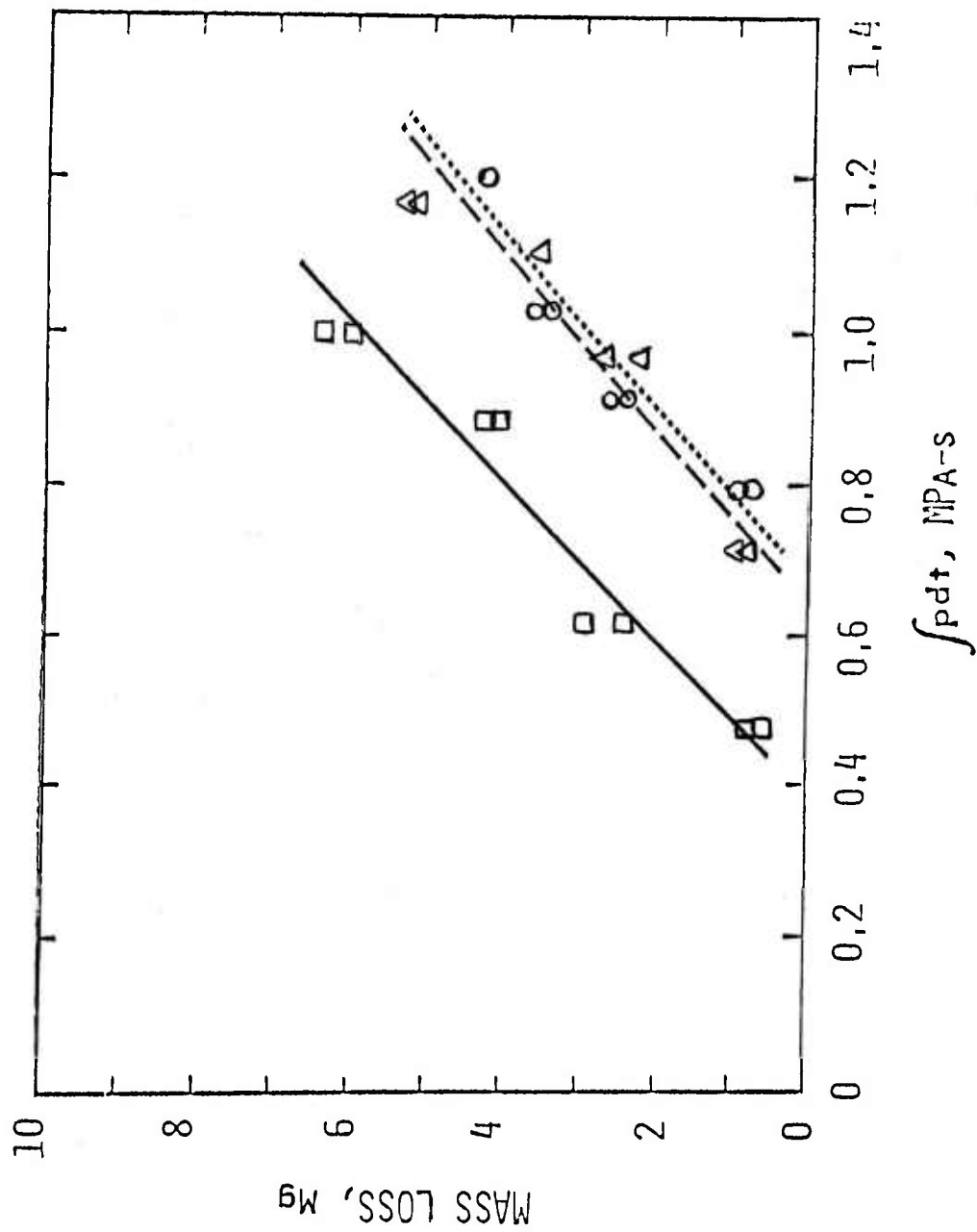
SHAVINGS

PRIMER

Figure 2. Princeton vented combustor

20

Figure 3. Mass loss produced by double-base propellants

21
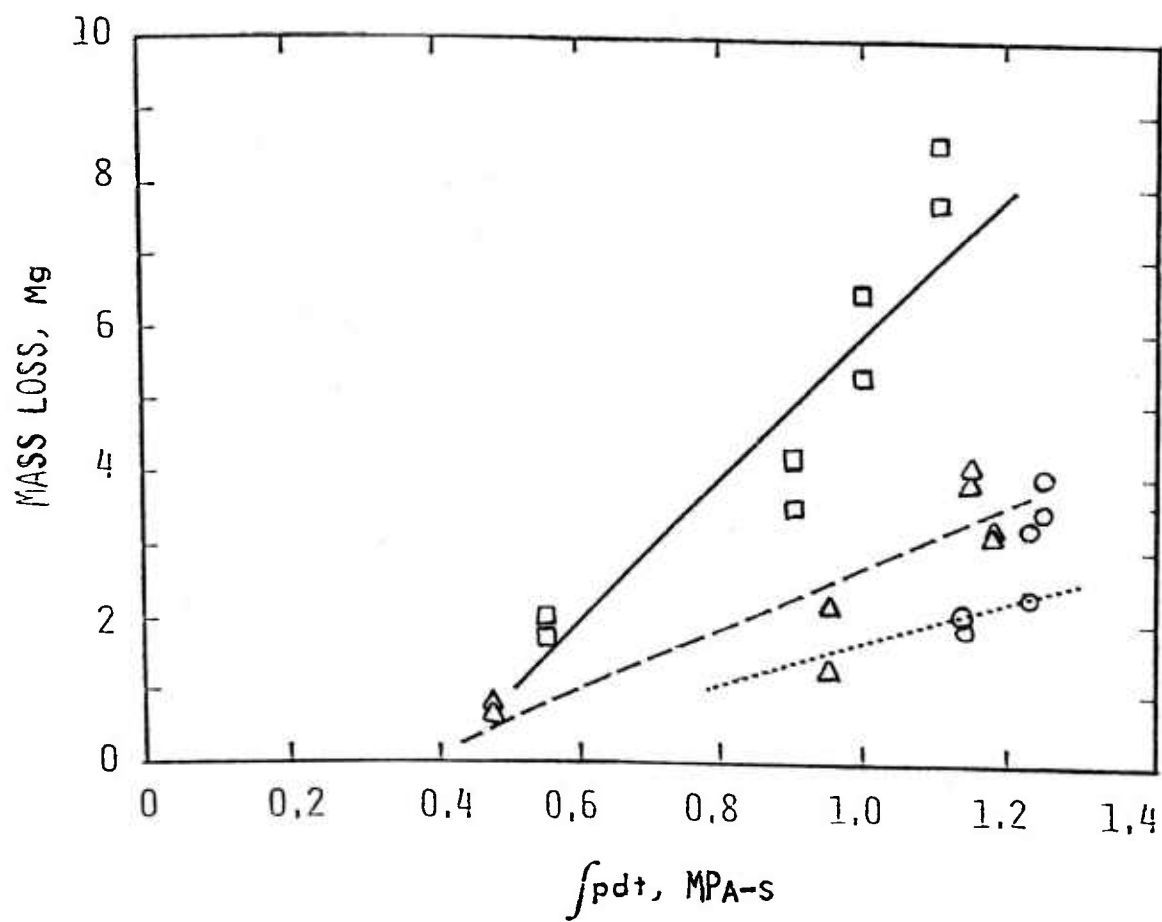
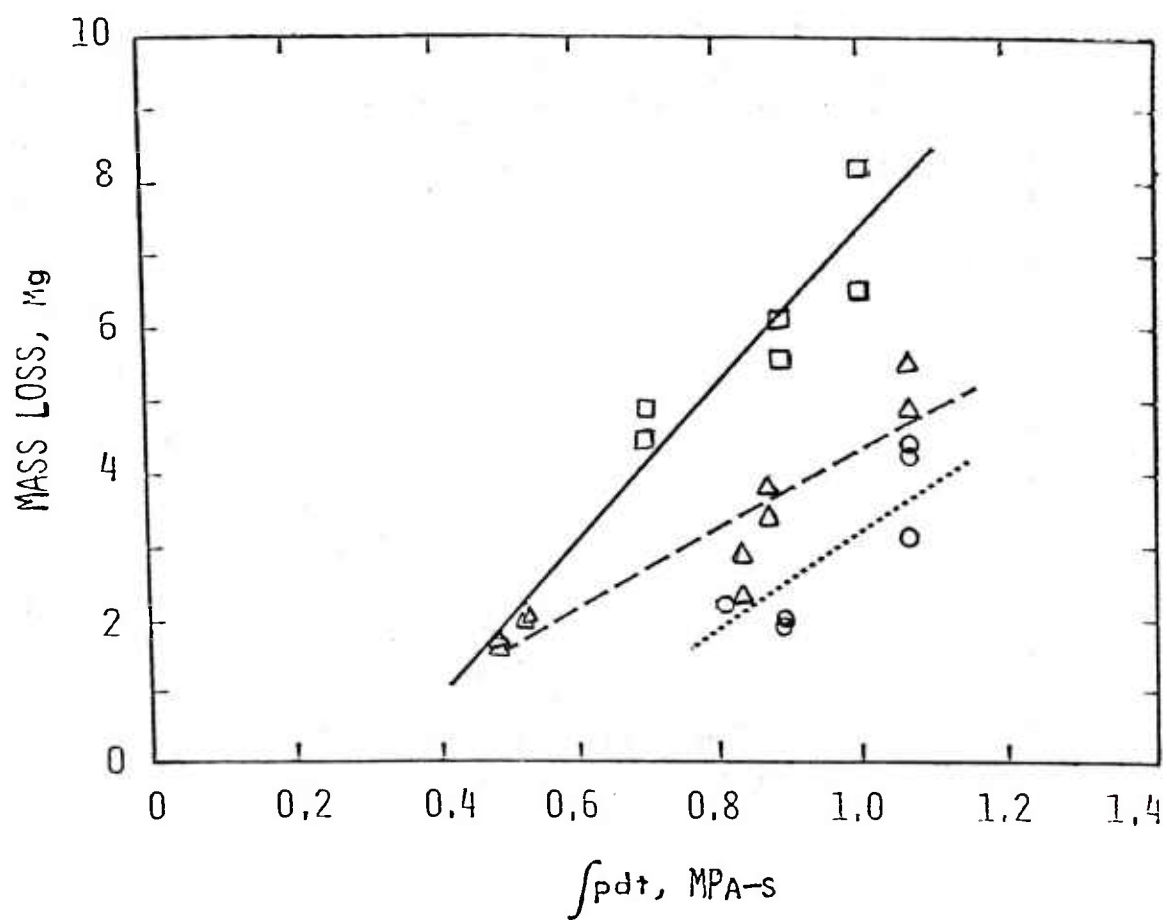Figure 4. Mass loss produced by triple-base propellants

MASS LOSS, Mg

10

8

6

4

2

0

0   0.2   0.4   0.6   0.8   1.0   1.2   1.4

$\int p\, dt$, MPA-s

Figure 5.   Mass loss produced by nitramine (RDX)
            containing propellants
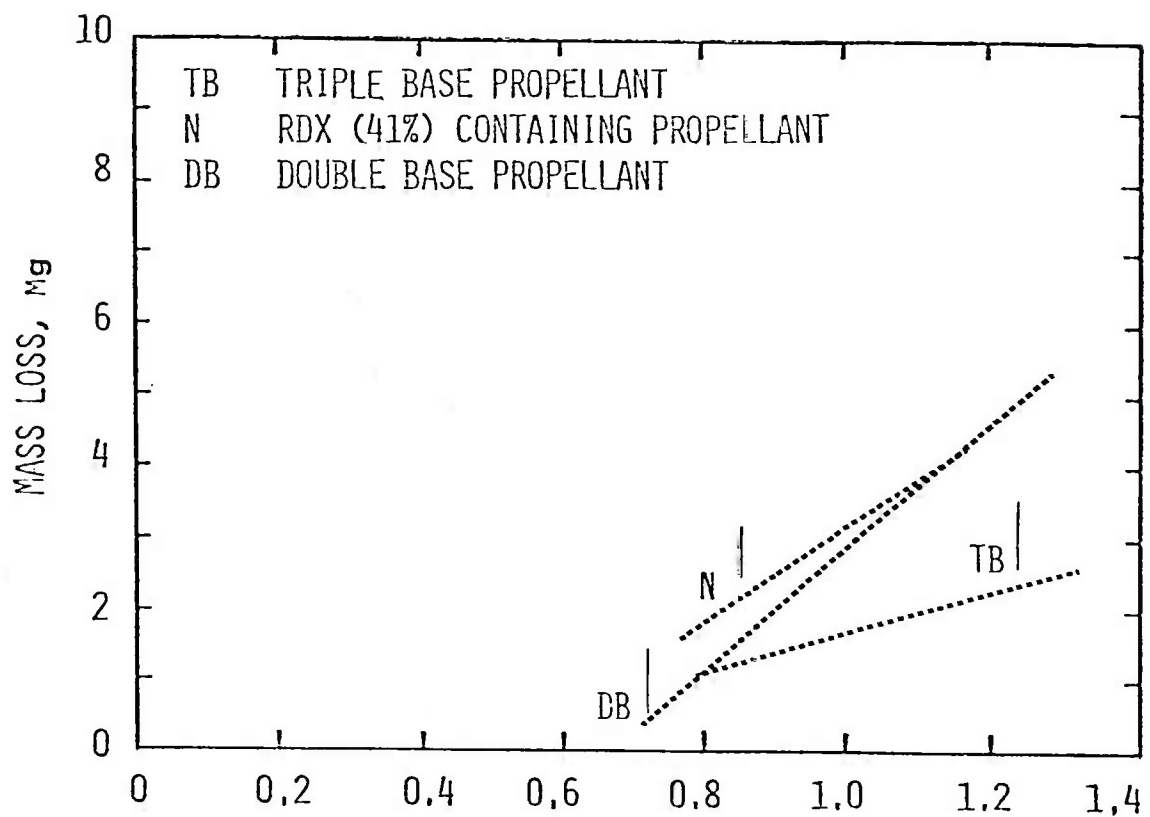
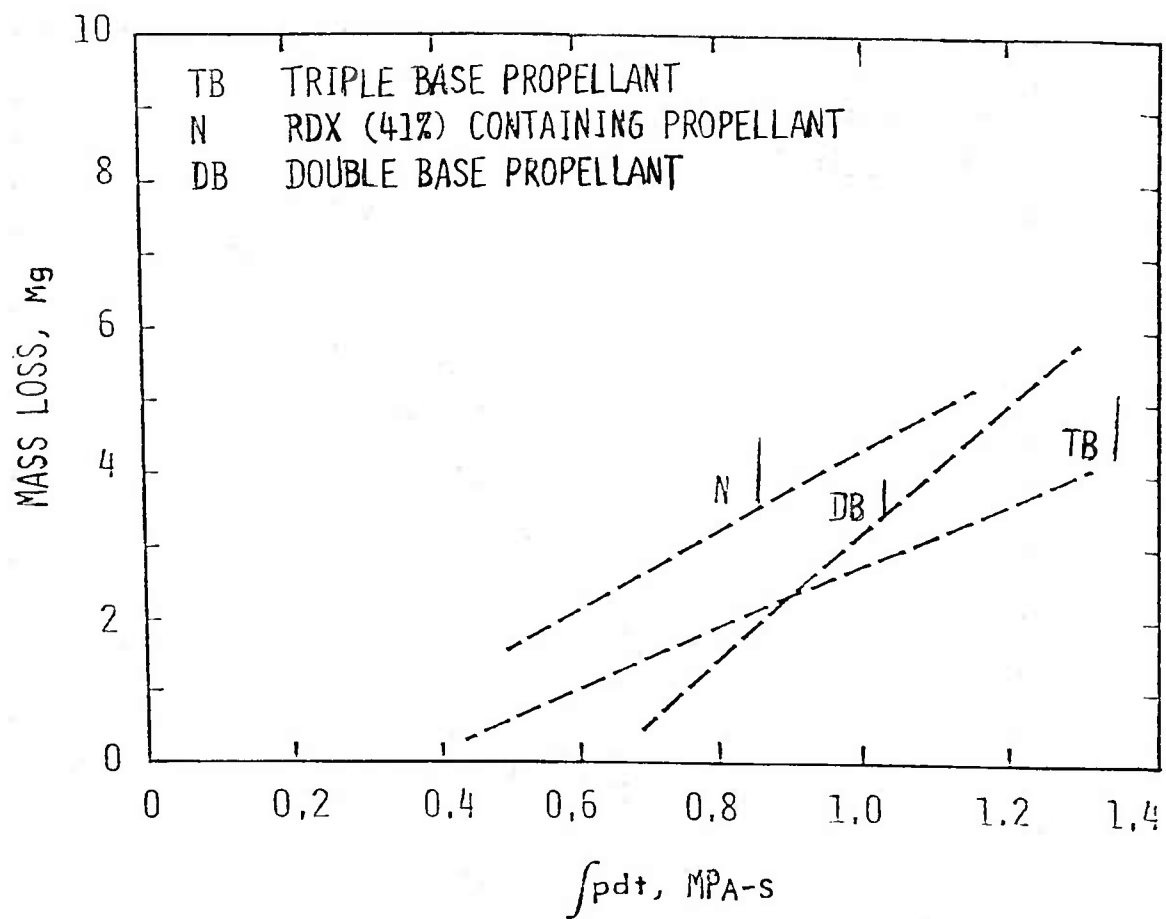Figure 6.   Comparison of mass loss produced by nominal
            2700 K propellants

Figure 7. Comparison of mass loss produced by nominal
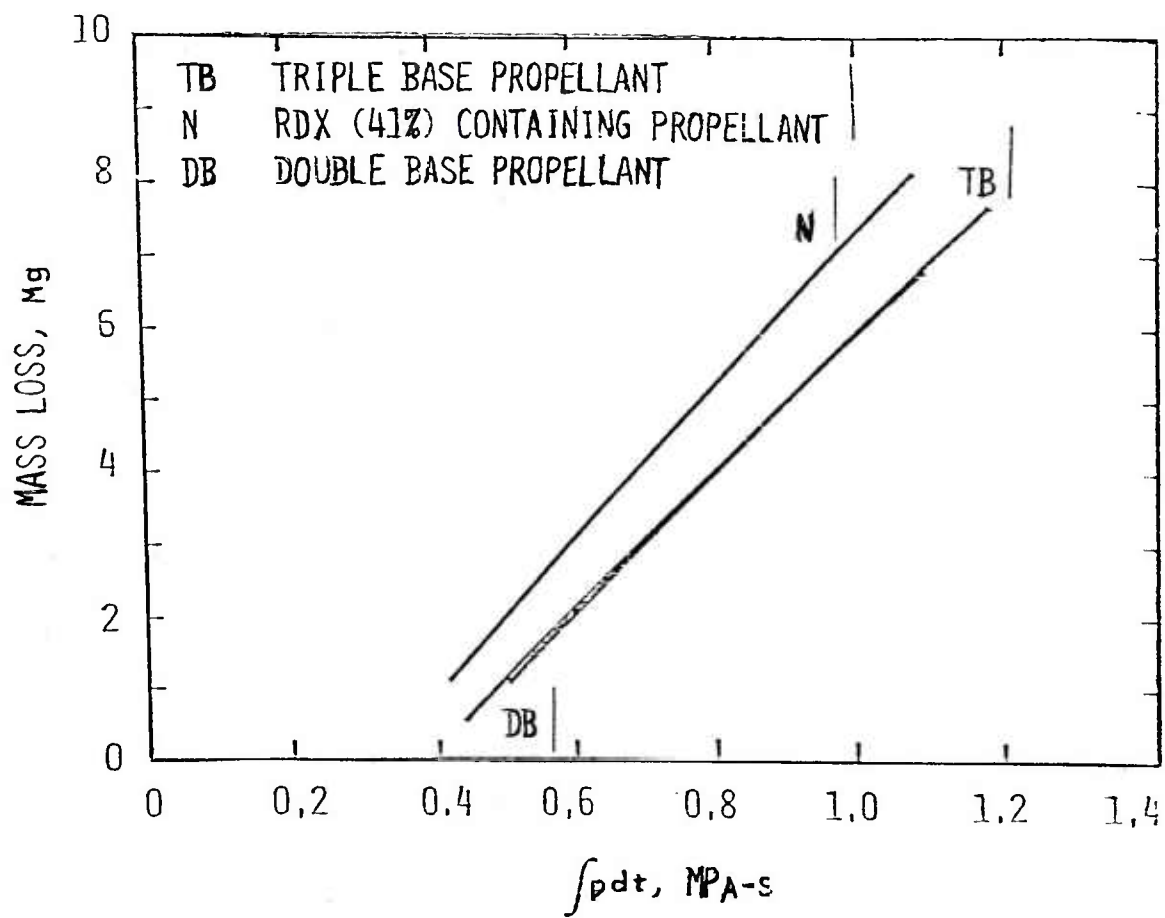3000 K propellants

25

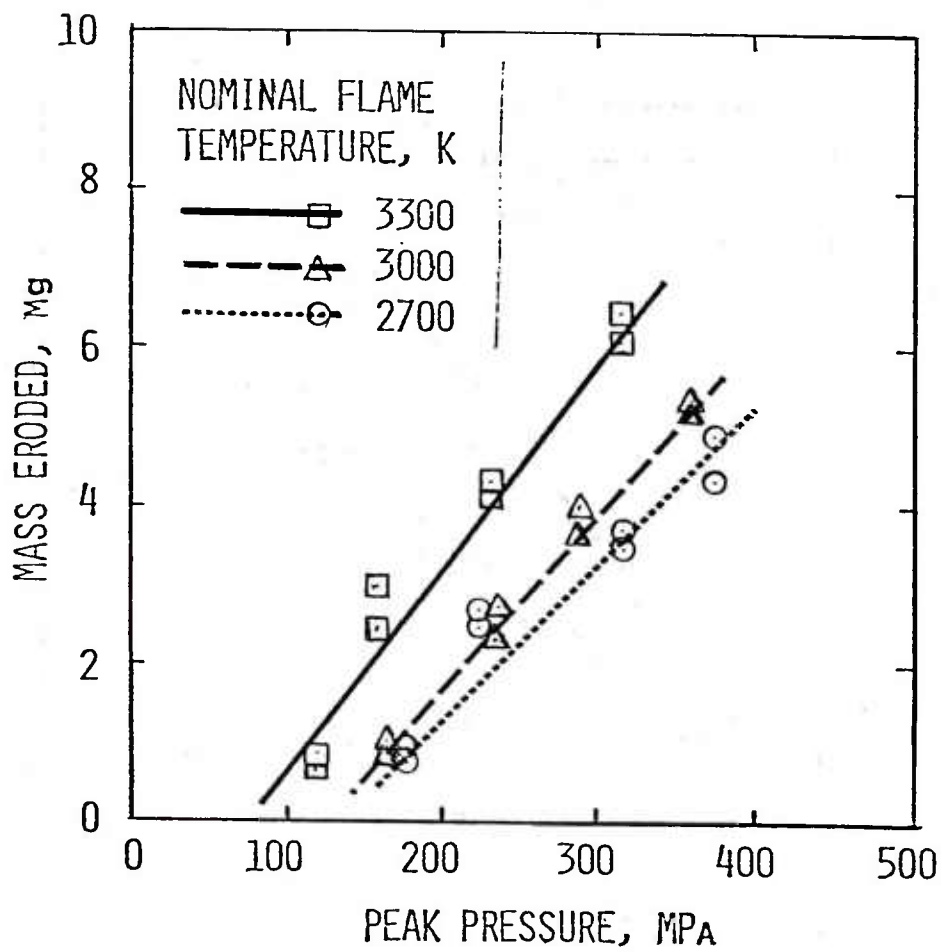Figure 8.   Comparison of mass loss prcduced by nominal
3300 K propellants

Figure 9. Mass loss versus peak chamber pressure
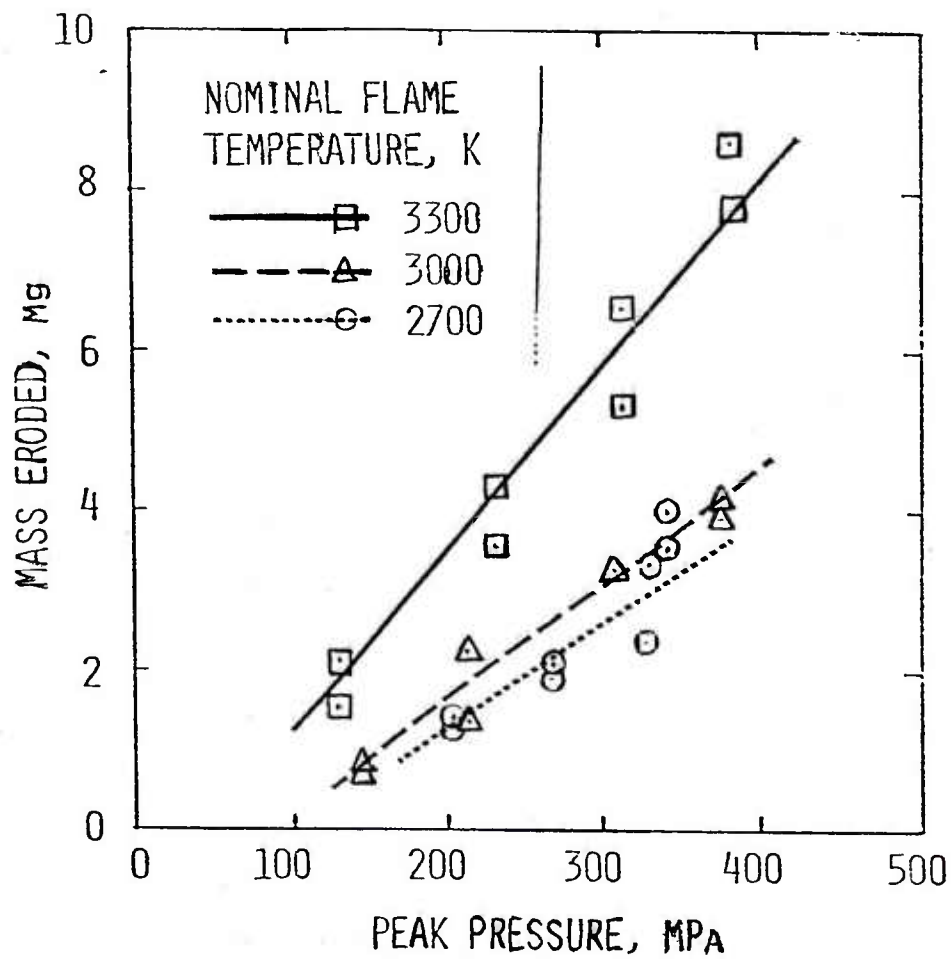produced double-base propellants

27

Figure 10. Mass loss versus peak chamber pressure
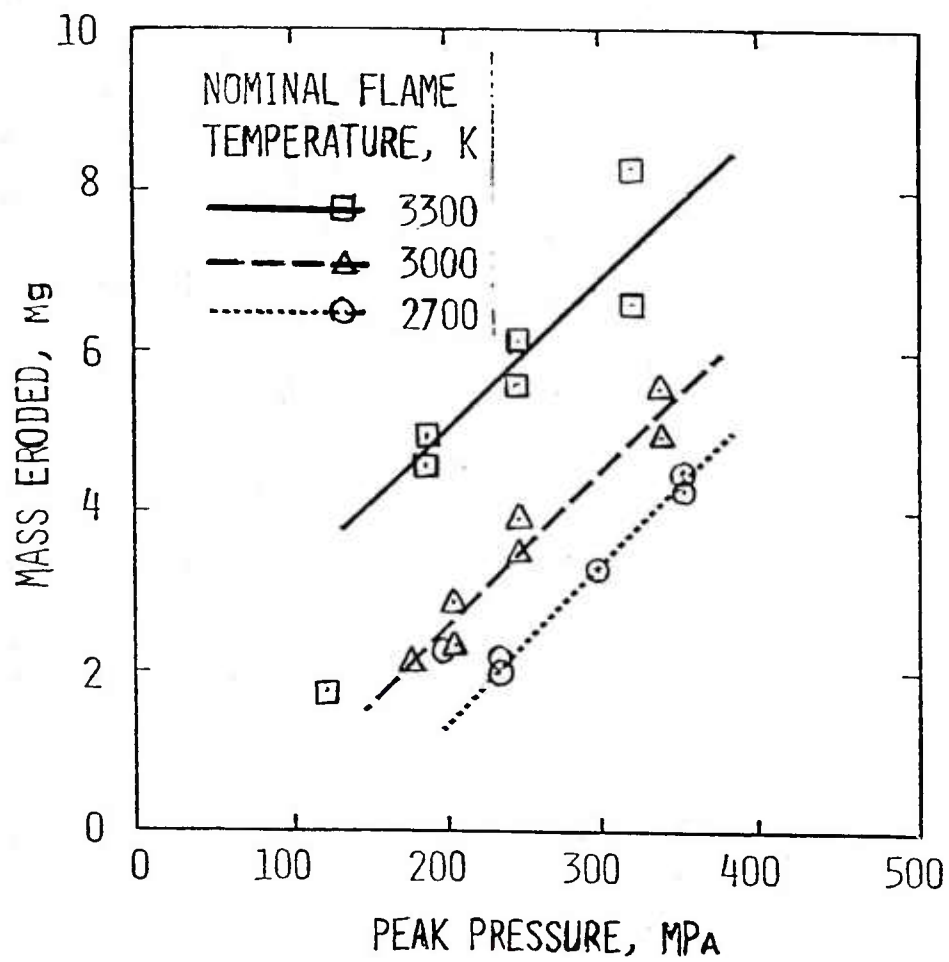produced by triple-base propellants

28

Figure 11.   Mass loss versus peak chamber pressure produced
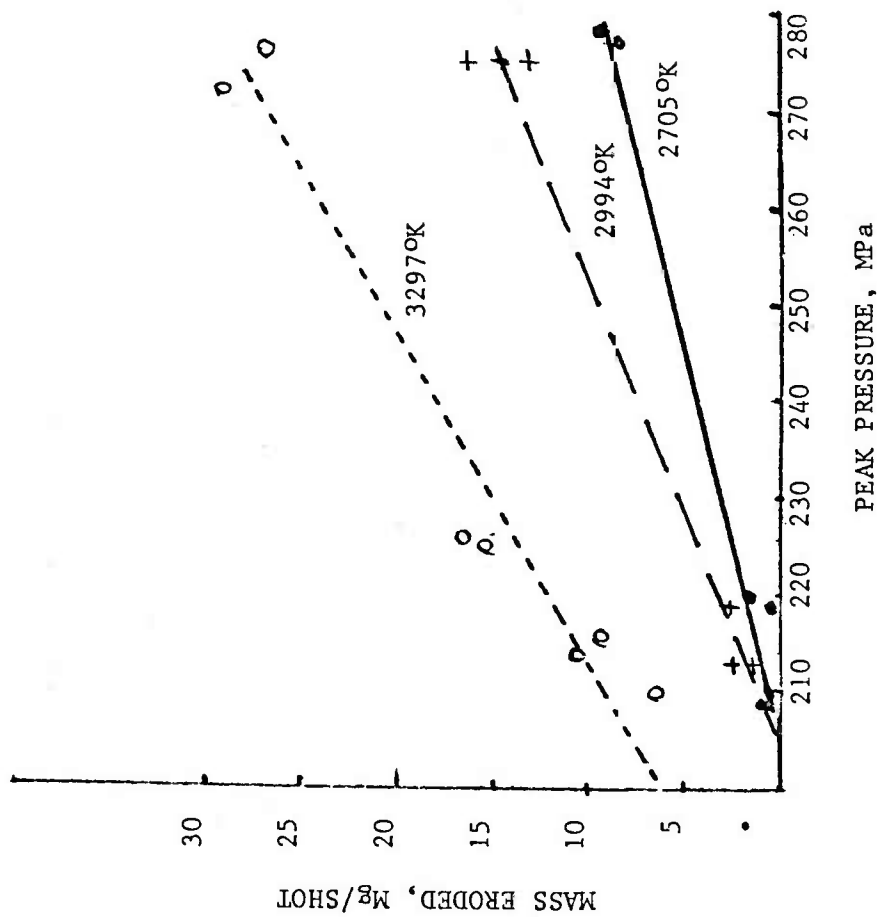by nitramine (RDX)-containing propellants

29

Figure 12. Mass loss versus peak pressure for double-base propellant

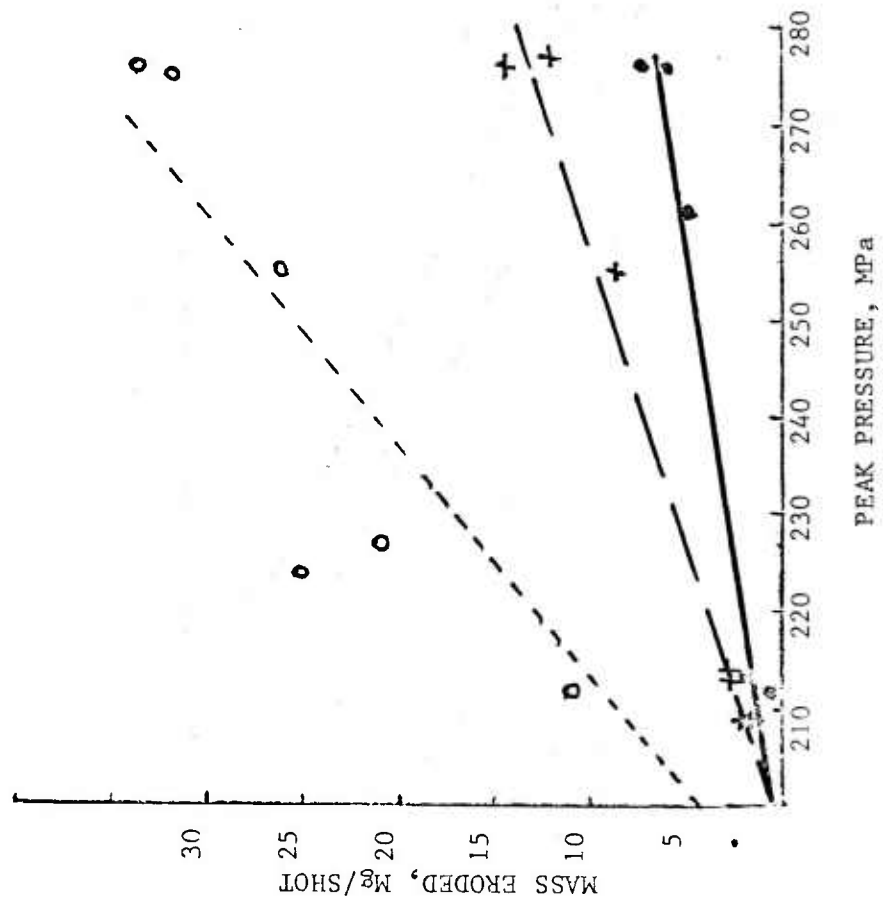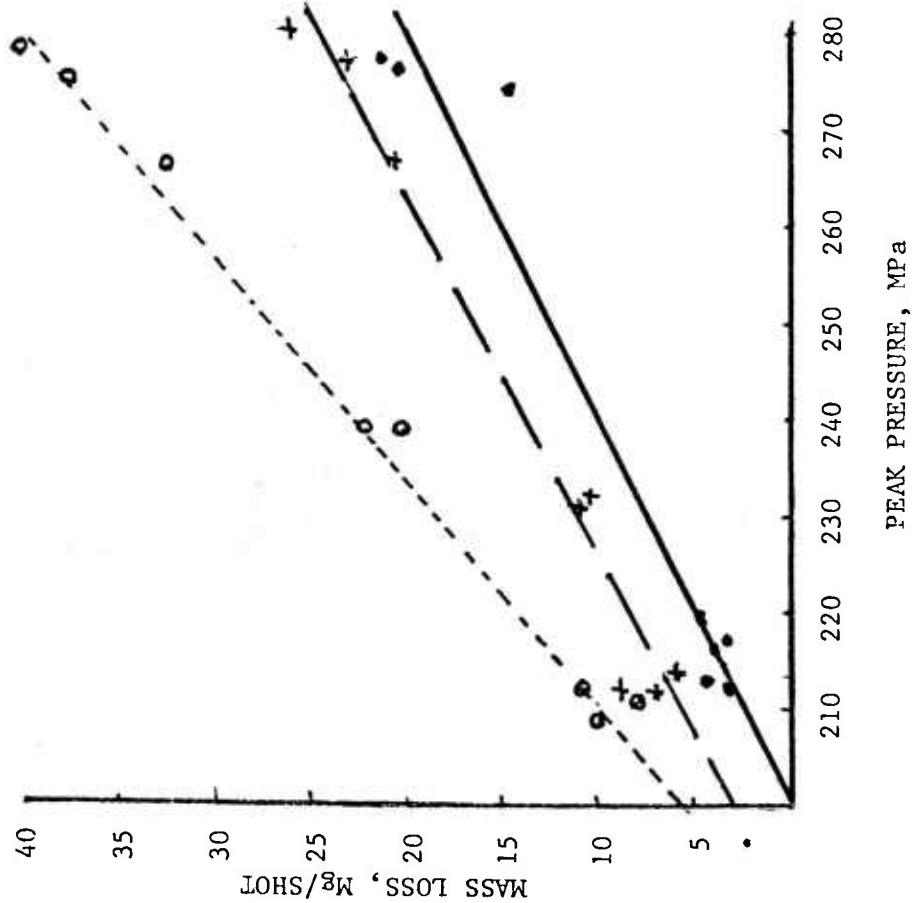Figure 13. Mass loss versus peak pressure for triple-base propellant

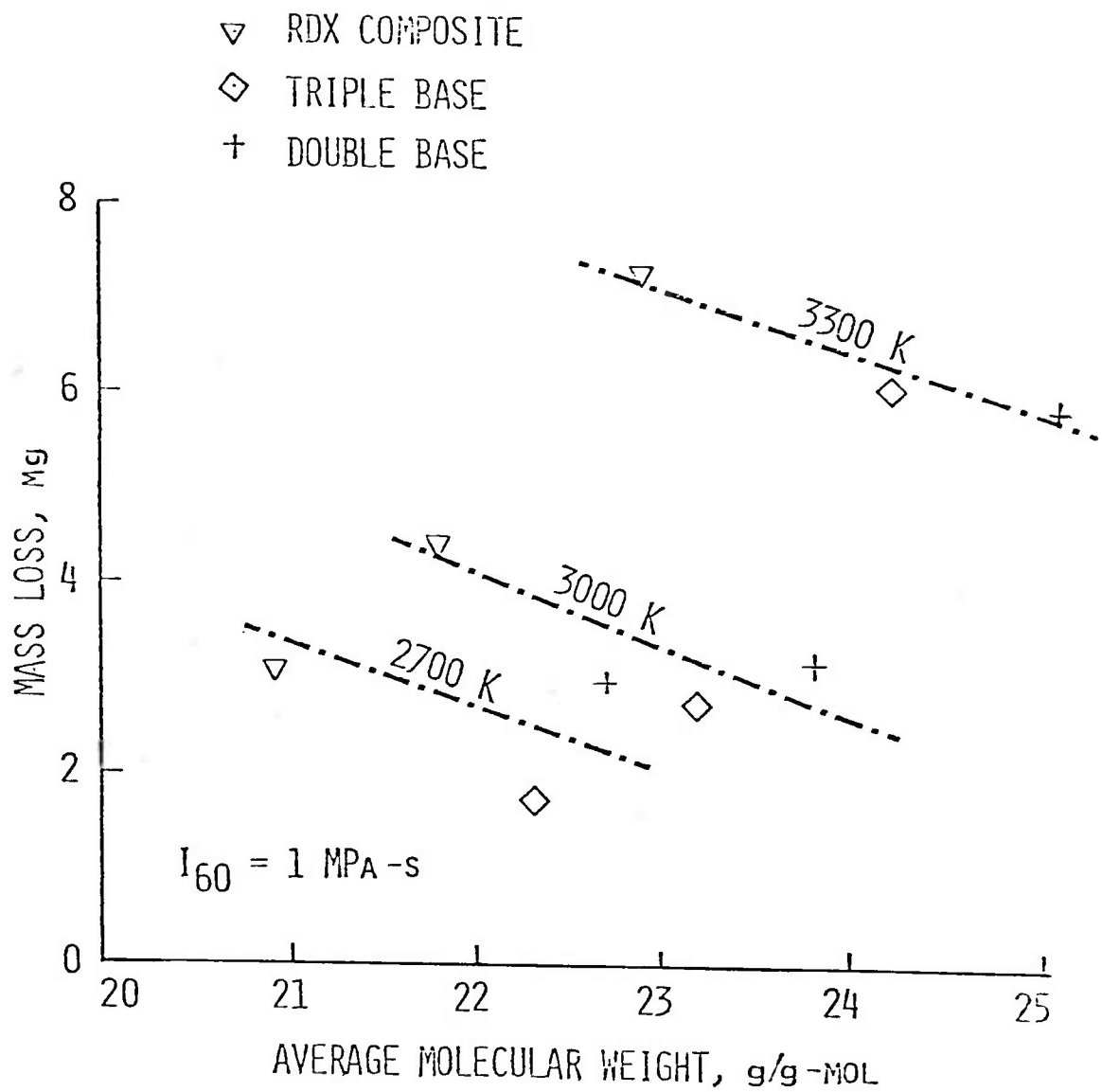Figure 14. Mass loss versus peak pressure for nitramine composite propellants

32

Figure 15.   Under constant p-t, integral and flame temperature mass loss increases as average molecular weight decreases

33

DISTRIBUTION LIST

Commander
U.S. Army Armament Research and
  Development Command
ATTN: DRDAR-LC, J. Frasier
        DRDAR-LCA, H. Fair
        DRDAR-LCA-G, E. Wurzel
                     B. Bernstein
                     K. Russell
                     D. Downs
                     L. Harris
                     A. Bracuti (10)
                     J. Lannon
                     L. Bottei
        DRDAR-LCE, J. Picard
                   A. Stearn
        DRDAR-LCU, A. Moss
        DRDAR-LCU-CA, D. Costa
        DRDAR-LCU-CT, E. Barrieres
        DRDAR-LCU-CP, R. Corn
        DRDAR-LCU-EE, D. Ellington
        DRDAR-LCS-D, K. Rubin
                     J. Houle
        DRDAR-QA, J Rutkowski
        DRDAR-SC, D. Gyorog
                  H. Kahn
                  B. Brodman
                  S. Cystron
                  L. Stiefel
        DRDAR-TSS   (5)
        DRDAR-MAD-C
        DRDAR-TSE-O
        DRDAR-GCL
Dover, NJ   07801

Project Manager, M60 Tanks
U.S. Army Tank & Automotive Command
28150 Dequindre Road
Warren, MI   48090

Project Manager
U.S. Army Armament Research and
  Development Command
Cannon Artillery Weapons Systems
ATTN: DRCPM-CAWS
Dover, NJ 07801

Chief
Benet Weapons Laboratory
U.S. Army Armament Research and
  Development Command
ATTN: DRDAR-LCB, I. Ahmad
                  T. Davidson
                  J. Zweig
                  G. Friar
                  J. Busuttil
                  W. Austin
                  R. Montgomery
                  J. Santini
       DRDAR-LCB-TL
Watervliet, NY 12189

Project Manager - M110E2
ATTN: J. Turkeltaub
       S. Smith
Rock Island, IL 61299

Project Manager - XM1 Tank
U.S. Army Tank Automotive
  Development Command
28150 Dequindre Road
Warren, MI 48090

Project Manager - SM1
Tank Main Armament Development Division
Dover, NJ 07801

Director
U.S. Army Materials and Mechanics
  Research Center
ATTN: J. W. Johnson
       R. Katz
Watertown, MA 02172

Director
U.S. Army TRADOC Systems
  Analysis Activity
ATTN: ATAA-SL
White Sand Missile Range, NM   88002

Administrator
Defense Technical Information Center
ATTN: Accessions Division   (12)
Cameron Station
Alexandria, VA   22314

Director
U.S. Army Materiel Systems Analysis Activity
ATTN: DRXSY-MP
Aberdeen Proving Ground, MD   21005

Commander
U.S. Army Armament Research and
  Development Command
Weapons Systems Concepts Team
ATTN: DRDAR-CLB-PA
APG, Edgewood Area, MD   21010

Director
Ballistics Research Laboratory
U.S. Army Armament Research and
  Development Command
ATTN: DRDAR-TSB-S
Aberdeen Proving ground, MD   21005

Commander
U.S. Army Armament Materiel
  Readiness Command
ATTN: DRSAR-LEP-L
Rock Island, IL   61299

Commander
U.S. Army Air Defense Center
ATTN: ATSA-SM-L
Fort Bliss, TX   79916

Commander
Armaments Development and Test Center
ATTN: AFATL
Eglin AFB, FL   32542

Commander
U.S. Army Armor Center
ATTN: ATZK-XM1
Fort Knox, KY 40121

President
U.S. Army Maintenance
    Management Center
Lexington, KY 40507

President
U.S. Army Armor and Engineering Board
Fort Knox, KY 40121

Commander
U.S. Army Field Artillery School
ATTN: J. Porter
Fort Sill, OK 73503

Headquarters
Office of the Deputy Chief of Staff for
  Research, Development, & Acquisition
ATTN: DAMA-ARZ
      DAMA-CSM
      DAMA-WSW
Washington, DC 20310

Director
U.S. Army Research Office
ATTN: P. Parrish
      E. Saibel
      R. Husk
      D. Squire
P.O. Box 12211
Research Triangle Park, NC 27709

Commander
U.S. Naval Ordnance Station
ATTN: L. Dickinson
      S. Mitchell
Indian Head, MD 20640

Commander
U.S. Naval Surface Weapons Center
ATTN: M. Shamblen
       J. O'Brasky
       C. Smith
       L. Russell
       T. W. Smith
Dahlgren, VA 22448

Commander
U.S. Naval Ordnance Station
ATTN: F. Blume
Louisville, KY 40202

AFATL
ATTN: D. Uhrig
       O. Heiney
Eglin AFB, FL 32542

National Bureau of Standards
Materials Division
ATTN: A. W. Ruff
Washington, DC 20234

National Science Foundation
Materials Division
Washington, DC 20550

Battelle Columbus Laboratory
ATTN: G. Wolken
Columbus, OH 43201

Lawrence Livermore Laboratory
ATTN: J. Kury
       A. Buckingham
Livermore, CA 94550

Calspan Corporation
ATTN: G. Sterbutzel
       F. Vassallo
P.O. Box 235
Buffalo, NY 14221

Director
Chemical Propulsion Information Agency
Johns Hopkins University
ATTN: T. Christian
Johns Hopkins Road
Laurel, MD 20810

Commander
U.S. Army Missile Research and
  Development Command
ATTN: Technical Library
Redstone Arsenal, AL 35809

SRI International
Materials Research Center
Menlo Park, CA 94025

Commander
U.S. Army Test and Evaluation Command
ATTN: DRSTE-FA
      DRSTE-AR
      DRSTE-AD
      DRSTE-TO-F
APG, Edgewood Area, MD 21010

Director
U.S. Army Materiel Systems
  Analysis Activity
ATTN: J. Sperrazza
      D. Barnhardt, RAM Div.
      G. Alexander, RAM Div.
      Air Warfare Div.
      Ground Warfare Div.
      RAM Div.
      DRXSY-MP, H. Cohen
Aberdeen Proving Ground, MD 21005

Commander
U.S. Army Test and Evaluation Command
ATTN: DRSTE-CM-F
Aberdeen Proving Ground, MD 21005

Commander
U.S. Army Armament Materiel
  Readiness Command
ATTN: DRCPM-TM
Rock Island Arsenal, IL 61299

Commander
U.S. Army Yuma Proving Ground
ATTN: STEYP-MSA-TL
        STEYP-MTW   (3)
        STEYP-MTE
Yuma, AZ   85364

Director
U.S. Army Ballistic
  Research Laboratories
ATTN: DRDAR-BL, Dr. Eichelberger
        DRDAR-BLP, L. Watermeier
                   J. R. Ward
                   I. C. Stobie
                   I. W. May
                   J. M. Frankie
                   T. L. Brosseau
Aberdeen Proving Ground, MD   21005

Director of Defense Research
  and Engineering
ATTN: R. Thorkildsen
The Pentagon
Arlington, VA   20301

Defense Advanced Research
  Projects Agency
Director, Materials Division
1400 Wilson Boulevard
Arlington, VA   22209

Command
U.S. Army Materiel Development and
  Readiness Command
ATTN: DRCDMD-ST
5001 Eisenhower Avenue
Alexandria, VA   22333

Commander
U.S. Army Aviation Research and
  Development Command
ATTN: DRSAV-E
P.O. Box 209
St. Louis, MO   63166

Director
U.S. Army Air Mobility Research and
  Development Laboratory
Ames Research Center
Moffett Field, CA 94035

Commander
U.S. Army Research and
  Technology Laboratories
ATTN: R. A. Langsworthy
Fort Eustis, VA 23604

Commander
U.S. Army Electronics Research and
  Development Command
Technical Support Activity
ATTN: DELSD-L
Fort Monmouth, NJ 07703

Commander
U.S. Army Communications Research and
  Development Command
ATTN: DRDCO-PPA-SA
Fort Monmouth, NJ 07703

Commander
U.S. Army Missile Research and
  Development Command
ATTN: DRDMI-R
       DRDMI-YDL
Redstone Arsenal, AL 35809

Commander
U.S. Army Tank Automotive R&D Command
ATTN: DRDTA-UL
Warren, MI 48090

Princeton Combustion Research Labs, Inc.
ATTN: N. Messina
1041 U.S. Highway One North
Princeton, NJ 08540

Commander
U.S. Army Materiel Development and
  Readiness Command
ATTN: DRCLDC, T. Shirata
5001 Eisenhower Boulevard
Alexandria, VA 22333

Headquarters
Department of the Army
ATTN: DAMA-ARZ-A, M. Lasser
                    E. Lippi
Pentagon
Washington, DC 20301